Electrically controlled total internal reflection in nematic hybrid cells

Carlos I. Mendoza*
Instituto de Investigaciones en Materiales, Universidad Nacional Autónoma de México, Apartado Postal 70-360, 04510 México, D.F., Mexico

J. A. Olivares† and J. A. Reyes
Instituto de Física, Universidad Nacional Autónoma de México, Apartado Postal 20-364, 01000 México, D.F., Mexico
(Received 7 July 2004; published 16 December 2004)

In this work, we show theoretically how the trajectories of an optical beam propagating in a planar-homeotropic hybrid nematic crystal cell can be modified by applying a low frequency electric field perpendicular to the cell. We use a previously developed formalism for describing the propagation of a polarized beam through the cell. We include a low frequency electric energy for the calculation of the equilibrium orientational configurations of the director's field. The presence of the electric field gives rise to trajectories showing a nontrivial dependence of the beam's range and penetration length with the intensity of the applied electric field.

DOI: 10.1103/PhysRevE.70.062701 PACS number(s): 42.70.Df, 42.15.−i, 42.70.−a

Liquid crystals are materials that have anisotropic properties, in particular nematic liquid crystals are, from the optical point of view, uniaxial materials. By a proper treatment of the boundaries that confine the liquid crystal it is possible to achieve a configuration in which the orientation of the molecules changes continuously from one substrate to the other. In particular, when the average orientation of the molecules is perpendicular to the substrate where the beam is penetrating and parallel to the other one, the effective refractive index coupled to the beam's extraordinary polarization will decrease continuously [1]. This leads to a continuous bending of the rays toward the region of higher refractive index [2]. Even more, it was shown [1,3,4] that if the substrates have a refractive index larger than those of the nematic, this will lead to a bending trajectory inside the liquid crystal cell similar to a mirage effect in an isotropic medium.

On the other hand, the local orientational state of a liquid crystal can be modified by the application of low frequency fields. Therefore the local optical axis and its associated refractive index gradient can be modulated by the low frequency electric field. Then, it is possible to electrically control the penetration length, the path, and the range of the beam traveling inside a liquid crystal cell. This phenomenon can be used as the base for a beam steering device or a multiplexor device.

In this Brief Report we show the possibility to electrically control the range and the depth of penetration of a linearly polarized beam incident on a nematic hybrid cell when total internal reflection conditions are satisfied.

The system under study consists of a pure thermotropic nematic confined between two parallel substrates with refraction indices N_t and N_b, respectively, as depicted in Fig. 1. The cell thickness l, measured along the z axis, is small compared to the dimension L of the cell plates. The directors initial configuration is spatially homogeneous along the x-y plane and varies with z so that at the boundaries the director

$$\hat{\mathbf{n}} = (\sin\ \theta(z), 0, \cos\ \theta(z)) \tag{1}$$

satisfies the hybrid boundary conditions

$$\theta(z = 0) = 0,$$

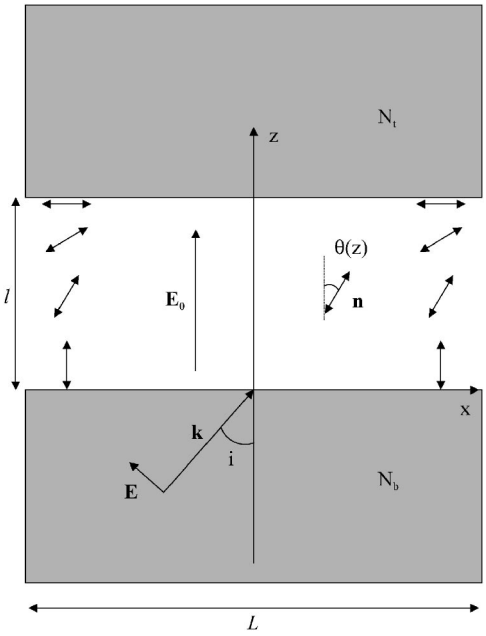

FIG. 1. Illustration of a pure thermotropic nematic confined between two parallel substrates. A TM mode is traveling along the hybrid nematic. $N_b, N_t > n_{\parallel}, n_{\perp}$.

*Corresponding author. Fax: +52 55 56161201. Email address: cmendoza@zinalco.iimatercu.unam.mx

†Present address: Centro de Investigación en Polímeros COMEX, Blvd. M. Avila Camacho 138, PH 1 y 2, Lomas de Chapultepec, CP 11560, México D.F., Mexico.

$$\theta(z=l)=\frac{\pi}{2}, \tag{2}$$

where $\theta(z)$ is the reorientational angle defined with respect to the z axis.

A low frequency uniform electric field E_0, parallel to the z axis, is applied. Then, the equilibrium orientational configurations of the director's field are specified by minimizing the total Helmholtz free energy functional as shown in Ref. [4]. Considering a uniaxial medium for which the dielectric tensor ε_{ij} has the general form

$$\varepsilon_{ij}=\varepsilon_{\perp}\delta_{ij}+\varepsilon_a n_i[\theta(z)]n_j[\theta(z)], \tag{3}$$

where $\varepsilon_{\perp}$ and $\varepsilon_{\parallel}$ are the dielectric constants perpendicular and parallel to the director and $\varepsilon_a \equiv \varepsilon_{\parallel}-\varepsilon_{\perp}$ is the dielectric anisotropy, and assuming the equal elastic constants approximation in which the elastic constants associated with the splay, twist, and bend deformations are described by a single constant K, then, the free energy functional turns out to be

$$F=\int_V dV\left[\frac{1}{2}K\left(\frac{d\theta}{dz}\right)^2-\frac{E_0^2}{8\pi}[\varepsilon_{\perp}+\varepsilon_a\cos^2\theta(z)]\right]. \tag{4}$$

The first and second terms of this equation represent the elastic and electromagnetic contribution of the free energy densities, respectively. The stationary configuration is then obtained by the corresponding Euler–Lagrange equation which reads

$$\frac{d^2\theta}{d\zeta^2}-q\sin 2\theta(\zeta)=0. \tag{5}$$

Here we have used the dimensionless variable $\zeta \equiv z/l$ and the parameter $q \equiv \tilde{\varepsilon}_a V^2/8\pi K$ which denotes the ratio between the electric energy and the elastic energy densities; in this sense, it measures the coupling between the electric field and the nematic. Here $\tilde{\varepsilon}_a$ is the low frequency dielectric anisotropy and $V \equiv E_0 l$ is the applied voltage.

An obliquely incident laser beam with P polarization (P wave), that is, contained in the incidence plane x-z, impinges the nematic with an incident angle i. The intensity of the beam is low enough so that it does not distort the nematic's configuration. The dynamics of this optical field is described by the corresponding Maxwell's equations which contain the dielectric tensor ϵ_{ij}, Eq. (3), and therefore depend on θ. The procedure to solve them has been carried out in detail for a hybrid cell similar to the one considered here [5], and it is found that there is a regime for the incidence angle i where the ray trajectory exhibits a caustic; that is, where it bends and remains inside the cell until it returns back toward the incidence substrate (see Fig. 2). This trajectory is given by [5]

$$\upsilon=\chi+\int_0^{\zeta} d\eta\frac{\varepsilon_{xz}\mp p\sqrt{\varepsilon_{\perp}\varepsilon_{\parallel}}/\sqrt{\varepsilon_{zz}-p^2}}{\varepsilon_{zz}}. \tag{6}$$

In this equation the dimensionless variable $\chi \equiv x/l$ has been introduced and $p \equiv N_b \sin i$ is the ray component in the x direction. υ is a constant that is determined by the incident point of the beam on the cell. The $\mp$ sign in Eq. (6) corresponds to a ray traveling with $\mathbf{k}$ in the $\pm z$ direction, that is, going from A to B and from B to C, respectively (see Fig. 2).

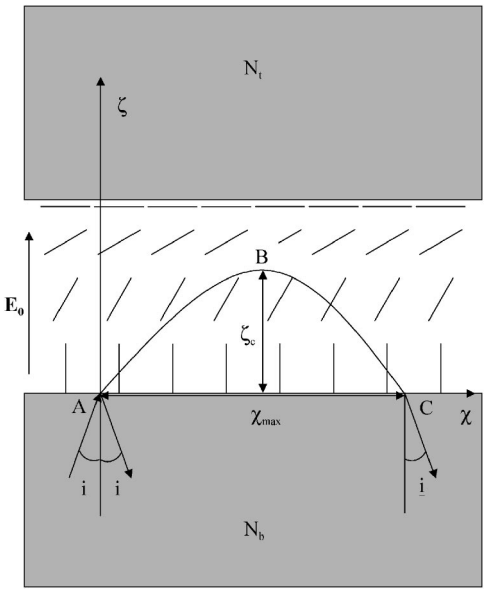

FIG. 2. Beam trajectory showing a caustic. ζ_c is the ray penetration.

In order to find the steady-state orientational configuration we need to solve Eq. (5) subject to the boundary conditions Eqs. (2). Numerically, we do this by using the "shooting" method [6], in which a search for initial conditions consistent with original boundary conditions is performed. The results for the orientational configuration are shown in Fig. 3. We see that as we increase the intensity of the electric field, the director tends to align to the z axis and it does not grow linearly with ζ as in the case of zero electric field.

As explained in Ref. [4], there are two regimes for i. The first one corresponds to $i-i_c<0$, with i_c a critical angle, where all the rays always reach the top substrate and part of the ray is transmitted to the top plate. On the other hand, the

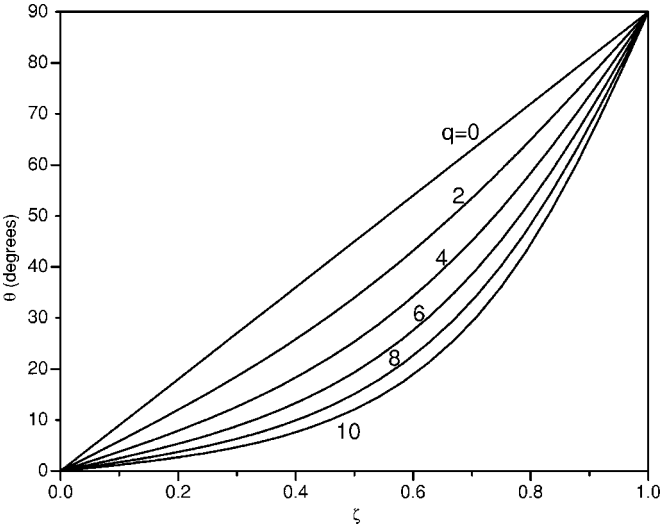

FIG. 3. Orientational angle of the director $\theta(z)$ as a function of ζ, for different values of $q=0,2,4,6,8$, and 10.

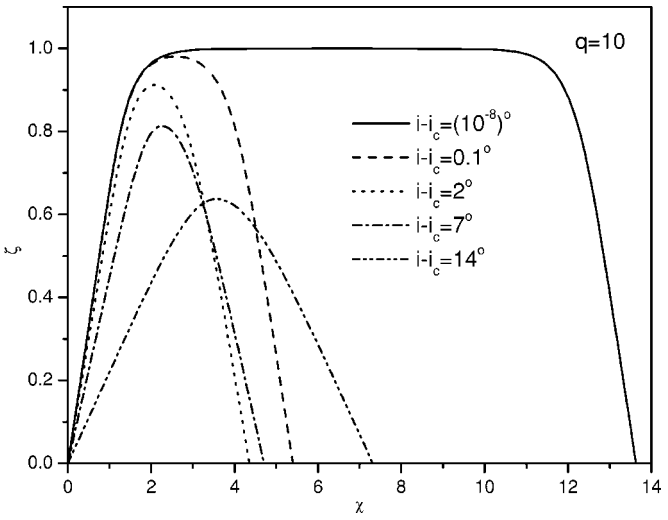

FIG. 4. Beam trajectories for $q=10$. $i_c=56.3°$.

second regime corresponds to $i-i_c>0$, namely, when the ray does not reach the top substrate and it is reflected back to the inside of the cell. Here we will be interested only in the second regime.

In Fig. 4 we show the trajectory of the beam, as calculated from Eq. (6), for $q=10$ and for different values of the incidence angle. The parameters used in this figure were $n_{\|}=1.735$, $n_{\perp}=1.506$, $\lambda=632.28$, and $N_b=N_t=1.81$. As we can see, the range of the beam does not necessarily decrease monotonically as we increase i, in contrast to the case of zero electric field.

The position of the caustic ζ_c, that is, the ray penetration length, always decreases when $i-i_c$ increases for all values of q, as it is shown in Fig. 5. The angle i_{c2}, for which the beam no longer penetrates the liquid crystal cell and at which it is reflected back to the lower substrate, is found from the condition $0=\arccos\sqrt{(p^2-\varepsilon_{\perp})/\varepsilon_a}$ and takes the value $i_{c2}=73.45°$ ($i-i_c=17.15°$).

The range of a bending ray $\chi_{\max}$ may be calculated from Eq. (6) with $\theta=0$. Figure 6 shows the range of the beam

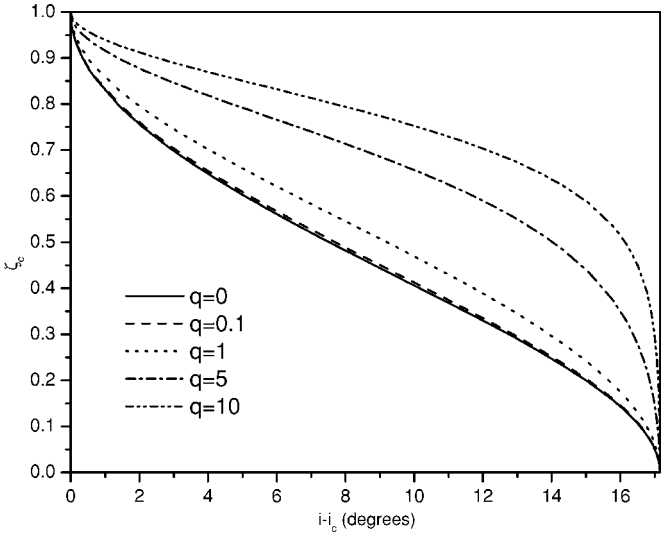

FIG. 5. Position of the caustic ζ_c as a function of the (shifted) angle of incidence $i-i_c$, for different values of q.

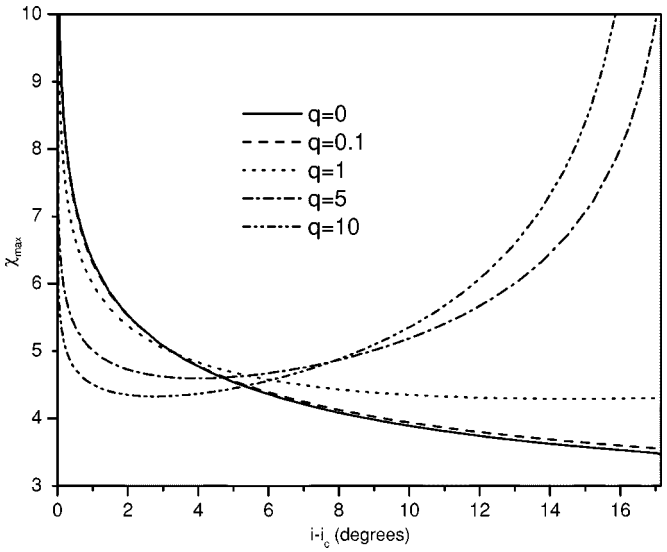

FIG. 6. Dimensionless range of a bending ray $\chi_{\max}$ as a function of the (shifted) angle of incidence $i-i_c$, for different values of q.

trajectory as a function of the (shifted) angle of incidence $i-i_c$. Two different kinds of behavior can be seen. For values of q close to zero, the range decreases monotonically with $i-i_c$, but for larger values of q, the range, first decreases and then increases with $i-i_c$. In all cases, as we approach the critical angle i_c, the range diverges to infinity due to the $1/x$-type divergence in Eq. (6). In this critical case, the beam grasps the top substrate and continues propagating parallel to it. Also, for high values of q, as we approach i_{c2}, the range may reach very large values.

Finally, in Fig. 7 we show the range as a function of q for different values of the (shifted) angle of incidence, $i-i_c$. We observe a complex behavior: For i close to i_c the range decreases but as we increase the value of i, the range may increase and then decrease (see, for example, the case $i-i_c=7$ in Fig. 7) while for larger values of i the range increases with q.

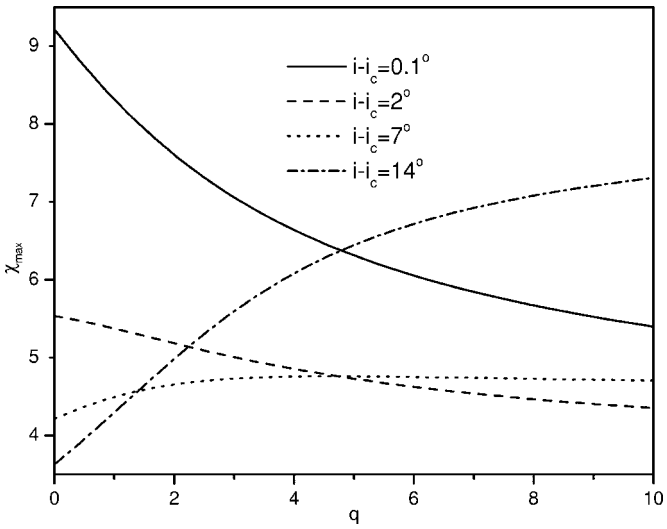

FIG. 7. Dimensionless range of a bending ray $\chi_{\max}$ as a function of q, for different values of the (shifted) angle of incidence $i-i_c$.

This peculiar dependence can be explained in terms of the coherence length of the field: $l_c = l/\sqrt{q}$ [7]. When $i \sim i_c$ the range is really large, furthermore, it diverges for $i = i_c$. Now, by increasing the field, the region where the refraction index is varying continuously is compressed to a smaller region located above the top substrate whose thickness is given by $l - l_c$. Thus the curved trajectory is reduced to a smaller region while in the rest of the nematic, the beam propagates following straight lines because there the nematic is almost uniformly aligned with E_0. This compression therefore reduces the range because the straight portions of the trajectory almost do not contribute to this range since for $i \sim i_c$ its component along χ is small. If otherwise i is farther from i_c, the range and the penetration length ζ_c are smaller than those for $i \sim i_c$. As discussed above, enlarging q leads also to a reduction of the continuously varying index region which now is smaller than that of the former case. However, the straight line portions of the trajectory are enlarged by increasing q contributing more to the range because its direction is nearer to χ.

In summary, we have calculated the optical path for a linearly polarized beam traveling in a hybrid nematic cell subject to a low frequency electric field perpendicular to the cell. We have shown that the range and the penetration length can be modified by varying the applied voltage. For example, for a typical nematic $\tilde{\varepsilon}_a = 13$ and $K = 10^{-11}$, then, for $q = 10$ the applied rms voltage is $V \simeq 1.2$ V. This yields for a cell with a thickness of 100 μm and for $i = i_c + 16° \simeq 69°$ a range of $\chi_{\max} \simeq 1$ mm and the corresponding penetration length of $\zeta_c \simeq 50$ μm. Therefore this effect could be used for the design of optical devices. For instance, by combining this hybrid cell with a hemisphere, the output beam can be steered by a refraction process at the hemisphere-air interface since the secondary reflection will leave the hybrid cell far from the center of the hemisphere. It should be remarked that it is expected that most of the energy will leave at the secondary reflection since the incident angle is far from the critical angle between the homeotropic layer and the substrate.

Another possible application consists in using this nematic cell as a multiplexor for switching among various optical fibers. Because the beam's range can be electrically controlled, the cell can be used to locate the outgoing beam in various cells' positions where some optical fibers were previously coupled. It should be remarked that the beam's output angle does not change by varying the applied voltage, simplifying considerably the optical coupling procedure with the exit fibers.

This work was supported in part by Grant No. CONACyT 41035 and DGAPA-UNAM Project No. IN110103-3.

[1] I.-C. Khoo, *Liquid Crystals: Physical Properties and Nonlinear Optical Phenomena* (Wiley, New York, 1994).
[2] M. Born and E. Wolf, *Priciples of Optics* (Cambridge University Press, Cambridge, U.K., 1999).
[3] M. Warenghem, M. Ismaili, and D. Hector, J. Phys. III **2**, 765 (1992); F. Simoni, F. Bloisi, L. Vicari, M. Warenghem, M. Ismaili, and D. Hector, Europhys. Lett. **21**, 189 (1993).
[4] J. A. Olivares, R. F. Rodriguez, and J. A. Reyes, Opt. Commun. **221**, 223 (2003).
[5] J. A. Reyes and R. F. Rodriguez, Mol. Cryst. Liq. Cryst. **317**, 135 (1998).
[6] William H. Press, Brian P. Flannery, Saul A. Teukolsky, and William T. Vetterling, *Numerical Recipes in Fortran*, 2nd ed. (Cambridge University Press, Cambridge, U.K., 1992).
[7] P. G. de Gennes and J. Prost, *The Physics of Liquid Crystals* (Clarendon, Oxford, 1993).